

Mass-spectrometric Study of the Vaporization of Magnesium Oxide from Magnesium Aluminate Spinel

Tadashi SASAMOTO,*† Hiroshi HARA,†† and Toshiyuki SATA

Research Laboratory of Engineering Materials, Tokyo Institute of Technology,
4259 Nagatsuta, Midori-ku, Yokohama 227

(Received November 7, 1980)

The partial vapor pressures of Mg(g) over the spinel solid solution system, $\text{MgO} \cdot n\text{Al}_2\text{O}_3$ ($n=1.0, 2.0$, and 2.8), have been measured by the mass-spectrometric Knudsen-cell method. In the temperature range from 1850 to 2300 K, the pressures are described by these equations:

$$\log[P(\text{Mg,g}) \text{ over } 1.0\text{-spinel/atm}] = 7.72 \pm 0.24 - (26900 \pm 490)/T,$$

$$\log[P(\text{Mg,g}) \text{ over } 2.0\text{-spinel/atm}] = 7.72 \pm 0.32 - (27400 \pm 670)/T,$$

$$\log[P(\text{Mg,g}) \text{ over } 2.8\text{-spinel/atm}] = 7.78 \pm 0.42 - (27900 \pm 1220)/T.$$

These observed values were discussed in comparison with the calculated ones obtained by an approximate thermodynamic treatment of an ionic solid solution with composition-dependent vacancies.

In a previous paper¹⁾ one of the present authors (T. Sata) reported that the vaporization of a magnesia component from spinels, $\text{MgO} \cdot 0.9\text{Al}_2\text{O}_3$ and $\text{MgO} \cdot 2.8\text{Al}_2\text{O}_3$, proceeds in two stages: the initial stage with a constant rate before the free surface is covered with the corundum precipitating during the preferential vaporization of the magnesia component, and the second stage controlled by the diffusion of O^{2-} ions through the corundum layer. It was concluded that the vaporization rate at the initial stage was controlled by the decomposition reaction, the activation energies of which were 587 and 327 kJ/mol for $\text{MgO} \cdot 0.9\text{Al}_2\text{O}_3$ and $\text{MgO} \cdot 2.8\text{Al}_2\text{O}_3$ respectively.

The aim of the present study is to measure the equilibrium vapor pressures and vaporization coefficients of Mg(g) and the activities of the magnesia component in the spinel solid solution system, $\text{MgAl}_2\text{O}_4\text{--Al}_2\text{O}_3$, and to provide data for discussing the detailed mechanism of the vaporization of a defective spinel the vapor pressure of which is affected by vacancies induced by the dissolution of Al_2O_3 , and to compare the observed vapor pressures with those calculated by the approximate treatment of thermodynamics, considering the electrical neutrality condition and the vacancy concentrations.

Experimental

Instrument. The instrument used for the measurement of the vapor pressure was a JMS-01BK-type double-focussing mass spectrometer equipped with a Knudsen-cell ion source, which had been described by Watanabe *et al.*^{2,3)} The main advantages of this mass spectrometer in the Knudsen measurement are: (1) high resolution, (2) the two ion-detecting systems of the electrical and photographic methods, and (3) the facility of sample exchange.

The Knudsen cell assembly, the ion source, and the slit system are shown in Fig. 1. The Knudsen cells, made of tungsten, sometimes has a ThO_2 liner; they were about 10 mm in both inner diameter and height. The knife-edge effusion orifice of the W or ThO_2 lid was 0.5 mm or

0.3 mm in diameter, so that the ratio of the effusion hole area to the sample surface area was less than about 1/400. The cell was set within the outer cell by means of the three legs and indirectly heated by the radiation from the outer cell, which was heated by electron bombardment. Although the temperature gradient in the cell was not checked, it must have been sufficiently small because the cell was set in an outer cell as a thermal block and the positions of the W-filaments for the electron bombardment were carefully regulated. The cell temperature was measured both with the optical pyrometer, which was sighted into the orifice of the cell through a quartz window, and with a W-5%Re/W-26%Re thermocouple positioned under the bottom of the cell. The calibration for the thermocouple was carried out by comparison with the temperature of the cell with a graphite liner measured by the pyrometer calibrated against the standard lamp and by taking advantage of the plateau of the ion intensity on the basis of the constancy of the vapor pressure at the melting points of several high-purity metals. The estimated uncertainty of the determined temperature was less than $\pm 1\%$.

The resolving power, $M/\Delta M$, measured using the peaks of two silver ions, $^{107}\text{Ag}^+$ and $^{109}\text{Ag}^+$, was about 2600 for

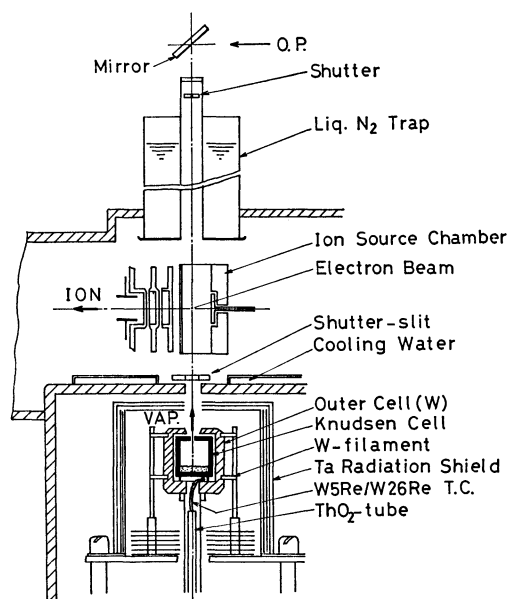


Fig. 1. Mass spectrometer with Knudsen-cell ion source.

† Present address: Tokyo National Technical College, 1220-2 Kunugida, Hachioji, Tokyo 193.

†† Present address: The Institute of Public Health, 4-6-1 Shirokanedai, Minato-ku, Tokyo 108.

the main slit width of 30 μm . It was enough for separating peaks of metal ions from the background peaks of hydrocarbon caused mainly by the decomposition of the diffusion oil. Since the shutter effect for permanent gases like oxygen was difficult to be obtained because of the imperfection of the slit mechanism and the insufficient evacuating ability, it was not possible for such a permanent gas to be distinguished from non-condensable residual gases in the source region of the mass spectrometer. The partial pressures of O_2 and O , therefore, could not be measured in this experiment.

The operational conditions of the ion source were as follows: ionization potential, 30 eV; ionization current, 500 μA ; ion-accelerating voltage, 7.8 kV, and temperature of ionization chamber, 250 $^\circ\text{C}$.

Procedure. About 350 mg of a sample (35–100 mesh grains) was placed in the cell with a weighed quantity of about 3 mg of the silver powder used as the reference material for vapor pressure. The Knudsen cell was then evacuated and heated by radiation from W-filaments up to 1400 K, followed by the electron bombardment. The vacuum was kept approximately in the 10^{-9} atm region at elevated temperatures.

When the temperature reached about 1300 K, the silver vapor beam effusing from the cell was ionized by electron impact with an energy of 30 eV, and the intensity of the $^{107}\text{Ag}^+$ ion beam was measured in order to determine the relation between the vapor pressure inside the cell and the intensity of the corresponding ion. After the silver had been completely vaporized, the temperature of the cell was rapidly raised up to a given temperature of from 1800 to 2300 K, and then we began to measure the Mg^+ ion intensity.

In the experiments using a photoplate as a detector, a few mg of copper were placed in the W-cell, together with a sample, as the reference material for both the vapor pressure and the calibration of the sensitivity of the photoplate (Ilford Q2). The conversion of the blackness of the spectrum on the plate into the relative ion intensity was carried out by means of Seidel's blackness *versus* relative ion-intensity curve, obtained by the two-line method using two isotope ions, $^{63}\text{Cu}^+$ and $^{65}\text{Cu}^+$. Sometimes, instead of copper, such stable background peaks as CO^+ , N_2^+ , O_2^+ , and CO_2^+ were also successfully used.

The conversion of the ion intensities to the absolute pressures of $\text{Mg}(\text{g})$ was calculated by using the following equations:⁴⁾

$$P(\text{Mg}) = K_1 K_2 I(^{24}\text{Mg}^+) T(\text{Mg}), \quad (1)$$

$$K_1 = \frac{P(\text{Ag}) r(^{107}\text{Ag})}{I(^{107}\text{Ag}^+) T(\text{Ag})}, \quad (2)$$

$$K_2 = \frac{\sigma(\text{Ag}) \Delta E(\text{Ag}^+) \gamma(\text{Ag}^+)}{\sigma(\text{Mg}) \Delta E(\text{Mg}^+) \gamma(^{24}\text{Mg}^+)}, \quad (3)$$

where K_1 and K_2 were the proportionality constants and P was the vapor pressure; I , the ion current; T , the absolute cell temperature; σ , the first ionization cross section given by Mann;⁵⁾ r , the isotopic abundance ratio; γ , the electron multiplier efficiency for ions in the first stage of the dynode, and $\Delta E = E - E_{\text{AP}}$, where E_{AP} was the appearance potential, and E , the energy of the ionization electron in eV. K_1 is called the calibration factor or the sensitivity factor.

Samples. Three kinds of single-crystal spinels with molar ratios of MgO to Al_2O_3 of 1.0 to 1.0 (called 1.0-spinel for simplicity), 1.0 to 2.0 (2.0-spinel), and 1.0 to 2.8 (2.8-spinel), prepared by the flame-fusion method, were used. The molar ratios of MgO to Al_2O_3 were determined by measuring the X-ray lattice parameters on the basis of the data of Shirasuga *et al.*⁶⁾ The lattice parameters calculated

from the (8.4.4), and (9.3.1) peaks were $a = 8.079 \text{ \AA}$ for the stoichiometric spinel, 1.0-spinel, $a = 7.992 \text{ \AA}$ for the 2.0-spinel, and $a = 7.978 \text{ \AA}$ for the 2.8-spinel.

Results

Vaporization of Spinel from Tungsten Cell. The intensities of ions formed from the gaseous species over the spinel/W-cell system were measured by the photographic detecting method. Figure 2 shows the time dependence of the ion intensities for the 2.8-spinel/W-cell system at 2180 K. Of these ions, the parent ones were determined from the appearance-potential data to be Mg^+ , WO_2^+ , WO_3^+ , WO_4^+ , Al^+ , and AlO^+ . This shows that the tungsten cell reacts with MgO to produce volatile W-oxides. The vapor pressure ratios, WO_2/WO_3 and AlO/Al , were about 2 and 27 respectively, these ratios agreed with those in the mass-spectrometric studies of the kinetics of the W-O_2 reaction by Berkowitz-Mattuck *et al.*⁷⁾ and Shissel *et al.*⁸⁾ and with those of the equilibrium vapor pressures in the $\text{W-Al}_2\text{O}_3$ system reported by Drowart *et al.*⁹⁾ Although the peak at $m/e = 40$ corresponding to $\text{MgO}(\text{g})$ was observed, the existence of molecular species $\text{MgO}(\text{g})$ was ambiguous because of the superposition of the $^{40}(\text{MgO})^+$ and $^{40}\text{Ca}^+$ peaks, as was pointed out by Drowart *et al.*¹⁰⁾ No other complex vapor, such as Al_2O , Al_2O_2 , and $(\text{WO}_3)_n (n > 4)$, was detected, since such vapors were present in quantities less than the detection limit of the instrument. The time dependences of the vapor-pressure ratios of $\text{Mg}(\text{g})$ to $\text{Al}(\text{g})$ at each temperature are shown in Fig. 3. These values lay approximately in the range from 10^2 to 10^3 .

Figure 4 plots the partial vapor pressures of $\text{Mg}(\text{g})$,

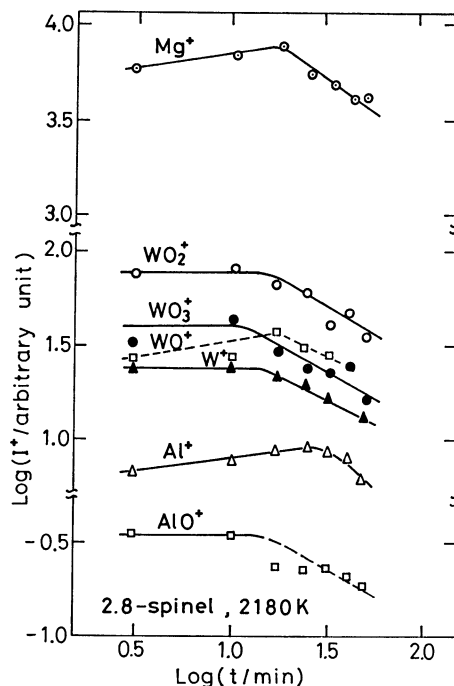


Fig. 2. Intensity of ions formed from gas species over the 2.8-spinel/W-cell system at 2180 K detected by a photographic plate.

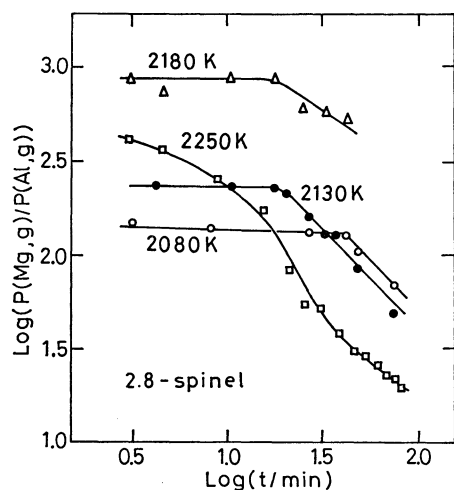


Fig. 3. Time-dependence of ratio of $P(\text{Mg},g)$ to $P(\text{Al},g)$ in the system 2.8-spinel/W-cell.

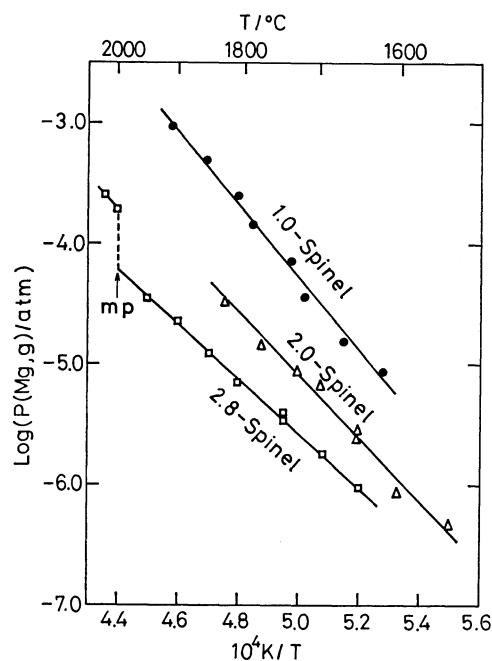
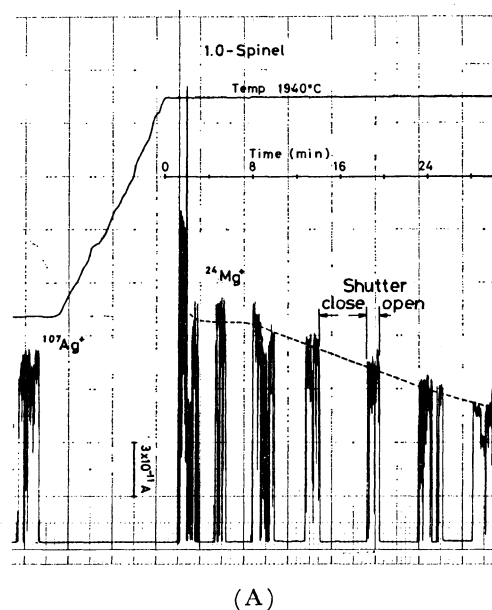


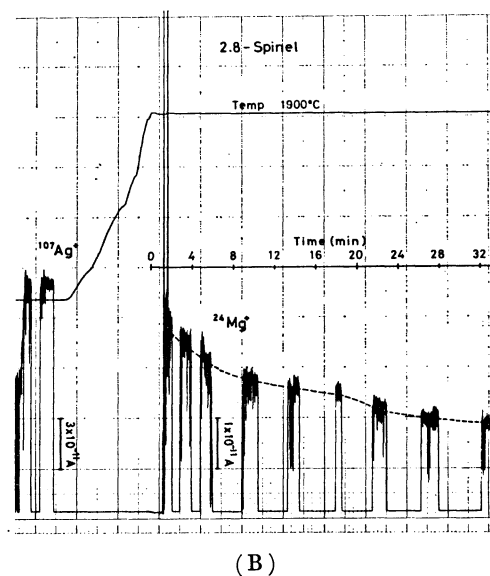
Fig. 4. Partial pressures of $\text{Mg}(g)$ over the n -spinel/W-cell system as a function of reciprocal absolute temperature.

$P(\text{Mg})$, as a function of $1/T$. From the slopes of these lines, the heats of vaporization for $\text{Mg}(g)$ over spinel were calculated to be 574, 494, and 436 kJ/mol for 1.0-, 2.0-, and 2.8-spinel respectively. The heat of vaporization for $\text{Mg}(g)$ over pure $\text{MgO}(s)$ was also determined to be 418 kJ/mol.

Vaporization of Spinel from W-Cell with a ThO_2 Liner. Figure 5 shows a typical time-dependence of the ion intensities of $^{24}\text{Mg}^+$ detected by means of a secondary electron multiplier (SEM) for 1.0- and 2.8-spinels. The appearance potential for Mg^+ obtained from the ionization efficiency measurement was 7.3 eV. This value means that the Mg^+ ion results from the simple ionization process. As can be seen in Fig. 5(A), a plateau of ion intensity was initially observed for the 1.0-spinel; a similar result was also obtained for the



(A)



(B)

Fig. 5. Typical examples of the time-dependence of the ion intensities of $^{24}\text{Mg}^+$ on (A) 1.0-spinel and (B) 2.8-spinel.

2.0-spinel. In the case of the 2.8-spinel, however, no plateau appeared and the ion intensity decreased with time, as is shown in Fig. 5(B). This was because the vaporizing surface was gradually covered with the precipitated alumina. Therefore, the ion intensities extrapolated to the intercept of time=0 were employed in the calculation of the equilibrium vapor pressure.

Figure 6 shows the van't Hoff plots of magnesium vapor pressure over the 1.0-spinel, $P(\text{Mg},g)$, calculated from Eq. 1 using the values of the ion intensity obtained by the step-by-step measurement in which the temperature was raised, step by step, at intervals of from 5 to 10 min. The vapor pressures obtained by both the step-by-step and isothermal measurements were in good agreement with each other. The values of $P(\text{Mg})$ over the 1.0-spinel were about half of that over pure MgO and were formulated by the least-squares method in the temperature range from 1850

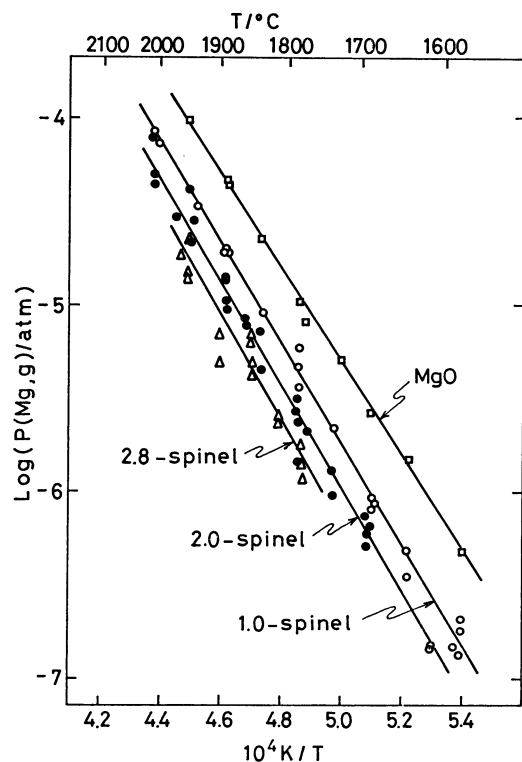


Fig. 6. Equilibrium vapor pressures of Mg(g) over the systems of n -spinel or magnesita/ThO₂-lined W-cell.

to 2300 K as follows:

$$\log[P(\text{Mg, g})/\text{atm}] = 7.72 \pm 0.24 - (26900 \pm 490)/T. \quad (4)$$

A similar temperature-dependence was obtained in the isothermal:

$$\log[P(\text{Mg, g})/\text{atm}] = 7.72 \pm 0.32 - (27400 \pm 670)/T. \quad (5)$$

For the 2.8-spinel, the initial values obtained in the isothermal experiment were plotted against $1/T$ for the reason described above, and the following equation was obtained:

$$\log[P(\text{Mg, g})/\text{atm}] = 7.78 \pm 0.42 - (27900 \pm 1220)/T. \quad (6)$$

The vapor pressures of $P(\text{Mg})$ over pure MgO(s) were given by this equation:

$$\log[P(\text{Mg, g})/\text{atm}] = 7.29 \pm 0.18 - (25200 \pm 310)/T. \quad (7)$$

Table 1 shows the activities of the magnesia component, $a(\text{MgO})$, as calculated by this equation:

$$a(\text{MgO}) = \frac{P(\text{Mg, g}) \text{ over } n\text{-spinel(s)}}{P(\text{Mg, g}) \text{ over MgO(s)}}, \quad (8)$$

using $P(\text{Mg, g})$ over MgO and the n -spinel given by Eqs. 4 to 7.

Using the Langmuir vapor pressures given by Sata *et al.*,¹⁾ the apparent vaporization coefficient of Mg(g) over the 1.0-spinel was given by this equation:

$$\log \alpha_v = \log[P_L(\text{Mg, g})/P_K(\text{Mg, g})], \quad (9)$$

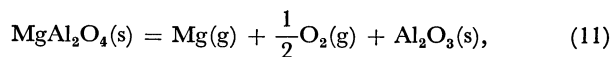
$$= -0.833 - (1330/T) \quad (10)$$

where P_L is the vapor pressure in the Langmuir free vaporization, and P_K the Knudsen vapor pressure, the equilibrium vapor pressure. From this equation, α_v at the melting point, $\approx 2100^\circ\text{C}$, was found not to be equal to unity; this was also observed in the experiment on the 2.8-spinel/W-cell system, as is

shown in Fig. 4. These results differed from those for α 's for MgO¹¹⁾ and MgCr₂O₄.¹²⁾

Discussion

If we use the phase diagrams of the MgO-Al₂O₃ system^{13,14)} and the JANAF Tables¹⁵⁾ for the following reaction:



and calculate the activities of the magnesium component, $a(\text{Mg})$, at 1800°C in a spinel solution on the basis of Raoult's law, we could expect the relation between $a(\text{MgO})$ and Al₂O₃ composition shown in Fig. 7. The measured values plotted in the figure, however, greatly deviated from the expected ones. This might come from the application of Eq. 11 as the vaporization reaction for this case; the Al₂O₃ on the right-hand side in Eq. 11 should be replaced by the spinel solid solution ($n > 1$), because MgAl₂O₄ and Al₂O₃ do not exist together, as can be seen from the phase diagram of Fig. 7. In fact, as is shown in Fig. 8, the $P(\text{Mg})$ values over MgAl₂O₄(s) calculated from the JANAF Tables¹⁵⁾ on the basis of MgAl₂O₄(s) = Mg(g) + 1/2O₂(g) + Al₂O₃(s) were smaller than our values and those of the literature.^{16,17)} Altman¹⁶⁾ suggested that the alumina produced by the vaporization reaction immediately formed a spinel solid solution with MgAl₂O₄ and decreased the activity of MgO.

Considering the above discussion, the desired $P(\text{Mg})$ over the single-phase of n -spinel, $P_{\text{Mg}/n\text{-spinel}}$, was determined by the following steps: first, $P(\text{Mg})$ over the two-phase region of the spinel-corundum, $P_{\text{Mg}/\text{two-phase}}$, was calculated using mainly the JANAF

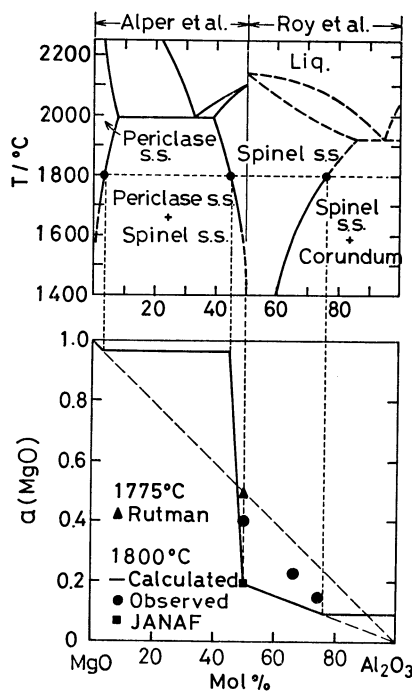


Fig. 7. Calculated relative vapor pressure of Mg(g) over the MgO-Al₂O₃ system assuming the Raoult's law.

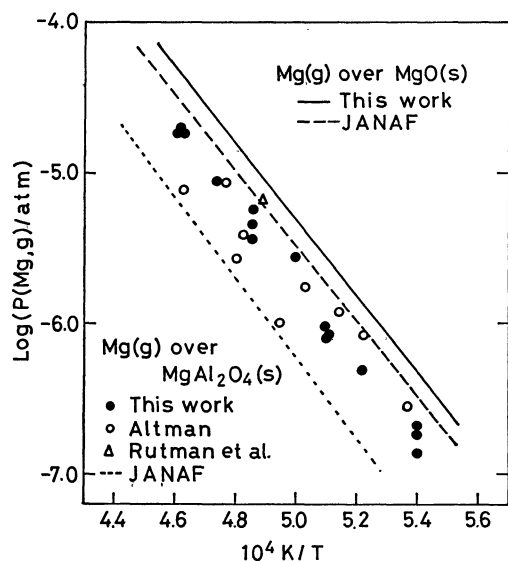
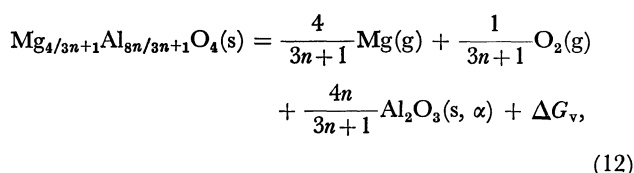


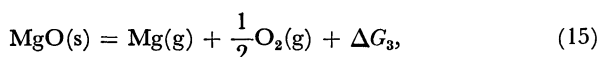
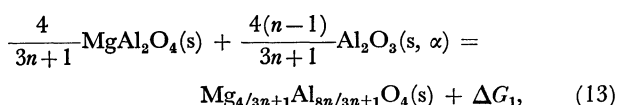
Fig. 8. Comparison of observed Knudsen vapor pressures of Mg(g) over 1.0-spinel with JANAF data.

Tables; next, the relative $P(\text{Mg})$ over the single n -spinel on an arbitrary basis, $P'_{\text{Mg}/n\text{-spinel}}$, was estimated as a function of the composition, n , by applying the method by Nakano¹⁸⁾ and Koumoto *et al.*¹⁹⁾ and finally, $P'_{\text{Mg}/n\text{-spinel}}$ was converted to $P_{\text{Mg}/n\text{-spinel}}$ using an appropriate correction factor, which was obtained by comparing $P'_{\text{Mg}/n\text{-spinel}}$ with $P_{\text{Mg}/\text{two-phase}}$ at the solubility limit of Al_2O_3 in the spinel.

The vaporization reaction in the two-phase region is as follows:



where α denotes alpha-type alumina, *i.e.*, corundum. This reaction is decomposed into the following three reactions:



where ΔG denotes the Gibbs energy. By combining Eqs. 13, 14, and 15, the following equation was derived:

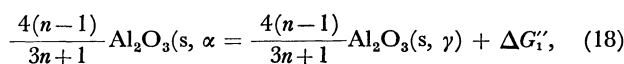
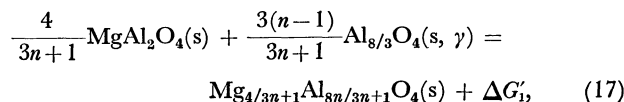
$$\frac{P_{\text{Mg}/n\text{-spinel}}}{P_{\text{Mg}/\text{MgO}}} = \exp\left[\frac{3n+1}{6}\left(\frac{\Delta G_1}{RT}\right) + \frac{2}{3}\left(\frac{\Delta G_2}{RT}\right)\right], \quad (16)$$

where $P_{\text{Mg}/n\text{-spinel}}$ and $P_{\text{Mg}/\text{MgO}}$ stand for the partial pressure of Mg(g) over the n -spinel(s) and MgO(s) respectively.

Here, ΔG_2 can be obtained from the JANAF Tables.¹⁵⁾ On the other hand, the ΔG_1 for the formation reaction of a solid solution in Eq. 13 is given as the sum of the following two Gibbs energies:

TABLE 1. ACTIVITIES OF MAGNESIA COMPONENT, $a(\text{MgO})$, IN THE SPINEL SOLID-SOLUTION SYSTEM $\text{MgO} \cdot n\text{Al}_2\text{O}_3$

Specimen	$a(\text{MgO})$			
	1700 °C	1800 °C	1900 °C	2000 °C
1.0-Spinel	0.376	0.408	0.444	0.481
2.0-Spinel	0.206	0.234	0.262	0.290
2.8-Spinel	—	0.154	0.177	0.200



$$\Delta G_1 = \Delta G'_1 + \Delta G'_2, \quad (19)$$

where γ stands for γ -type alumina.

Shirasuka *et al.*^{20,21)} have recently reported, on the basis of the DTA experiment, that the exsolution of alumina from the spinel body with $n=1.5$ —5.6 was exothermic. It is thought that this exothermic reaction resulted from the γ to α -transformation reaction, as is shown in Eq. 18.

The $\Delta G'_1$ in Eq. 18 can be obtained from the JANAF Tables. The $\Delta G'_1$ for Eq. 17 was obtained in the following manner. As the change in the volume of this reaction was very small (for examples, -0.16% for 3.0-spinel), the enthalpy change for the reaction was considered to be negligibly small. Therefore, $\Delta G'_1$ is reduced to:

$$\Delta G'_1 \simeq -T\Delta S_m, \quad (20)$$

where ΔS_m is the mixing entropy for Eq. 17. Here, ΔS_m is obtained by simple statistical thermodynamics on the assumption that the cations and cation vacancies are distributed randomly at tetrahedral and octahedral sites at a high temperature in the case of a spinel solid solution with the composition of $\text{MgO} \cdot n\text{Al}_2\text{O}_3 = (3n+1)/4\text{Mg}_{4/(3n+1)}\text{Al}_{8n/(3n+1)}\text{O}_4$. Let N_t be the total number of cation sites, and let N_{Mg} , N_{Al} , and N_v be the numbers of the Mg^{2+} , Al^{3+} , and cation vacancies respectively. Then, the following relationships hold:

$$\left. \begin{aligned} N_t &= 3N_A, \\ N_{\text{Mg}} &= \left(\frac{4}{3n+1}\right)\frac{N_t}{3}, \\ N_{\text{Al}} &= \left(\frac{8n}{3n+1}\right)\frac{N_t}{3}, \\ N_v &= N_t - N_{\text{Mg}} - N_{\text{Al}} = \left(\frac{n-1}{3n+1}\right)\frac{N_t}{3}, \end{aligned} \right\} \quad (21)$$

where N_A is Avogadro's constant. The number of distinguishable arrangements of cations and cation vacancies, W , is expressed as follows:

$$W = \frac{N_t!}{N_{\text{Mg}}! N_{\text{Al}}! N_v!}. \quad (22)$$

The contribution of mixing term to the entropy is expressed as:

$$S_c = k \ln W, \quad (23)$$

TABLE 2. GIBBS ENERGIES RELATING TO THE VAPORIZATION REACTION OF SPINELS
 AND THE PARTIAL PRESSURES OF Mg(g) OVER VARIOUS n -SPINELS

$T/^\circ\text{C}$	n at $T/^\circ\text{C}^a$	$\Delta G_1'$ for Eq. 17 ^b kJ/mol	$\Delta G_1''$ for Eq. 18 ^c kJ/mol	ΔG_2 for Eq. 14 ^c kJ/mol	$a(\text{MgO})$ from Eq. 16	$P(\text{Mg})$ over n -spinel atm
1500	1.67	-6.116	8.588	-35.12	0.242	1.86×10^{-8}
1600	2.14	-7.428	7.775	-35.68	0.224	1.00×10^{-7}
1700	2.95	-8.077	6.950	-36.30	0.205	4.49×10^{-7}
1800	4.26	-7.951	6.129	-36.98	0.188	1.73×10^{-6}
1900	6.81	-6.941	5.291	-37.73	0.180	6.08×10^{-6}

a) n in $\text{MgO} \cdot n\text{Al}_2\text{O}_3$ on the solubility limit line at temperatures in the first column. b) Calculated from Eq. 25. c) From JANAF Tables.

where S_c denotes the configurational entropy. The substitution of Eqs. 21 and 22 into Eq. 23 yields the desired equation:

$$\begin{aligned}
 S_c(n) &= -3R \left(\frac{N_{\text{Mg}}}{N_t} \ln \frac{N_{\text{Mg}}}{N_t} + \frac{N_{\text{Al}}}{N_t} \ln \frac{N_{\text{Al}}}{N_t} + \frac{N_v}{N_t} \ln \frac{N_v}{N_t} \right) \\
 &= \frac{-R}{3n+1} [4 \ln 4 + 8n \ln 8n + (n-1) \ln (n-1) \\
 &\quad - 3(3n+1) \ln 3(3n+1)], \quad (24)
 \end{aligned}$$

and thus:

$$\begin{aligned}
 \Delta G_1' &\approx -T \Delta S_m \\
 &= -T \left[S_c(n=n) - \frac{4}{3n+1} S_c(n=1) - \frac{3(n-1)}{3n+1} S_c(n=\infty) \right] \\
 &= \frac{-RT}{3n+1} [8n \ln 8n + (n-1) \ln (n-1) \\
 &\quad - 3(3n+1) \ln 3(3n+1) + 3.139n + 10.045]. \quad (25)
 \end{aligned}$$

The Gibbs energies of $\Delta G_1'$, $\Delta G_1''$, and ΔG_2 for the n -spinel on the solubility limit line at several temperatures between 1500 and 1900 $^\circ\text{C}$ are summarized in Table 2. From these Gibbs energies, and by applying Eq. 16, the ratios of P_{Mg} over the n -spinel(s) to P_{Mg} over $\text{MgO}(\text{s})$, i.e., $a(\text{MgO})$, were calculated. The partial pressures of $\text{Mg}(\text{g})$ over the n -spinel, calculated using this $a(\text{MgO})$ and JANAF data for $P(\text{Mg})$ over pure $\text{MgO}(\text{s})$, are also shown in the last column in Table 2 and graphically in Fig. 9.

The partial pressures of $\text{Mg}(\text{g})$ over the spinel solid solution in the single-phase region are given by the following equation:^{18,19)}

$$\begin{aligned}
 \ln P(\text{Mg}, \text{g})^{3/2} &= \ln \frac{4}{3(3n+1)} \left[\frac{n-1}{3(3n+1)} \right]^{-1/4} + C \\
 C &= \frac{h_{\text{MgO}} - K_{\text{Mg}} - 1/2 K_{\text{O}_2}}{RT}, \quad (26)
 \end{aligned}$$

where h_{MgO} is the enthalpy term and where K_{Mg} and K_{O_2} are constants independent of the composition. As it was assumed that a spinel solid solution is ideal; that $\Delta H_m \approx 0$, and that every vapor species behaves as a perfect gas, C should be constant. $P(\text{Mg})$ over n -spinel(s) in the single-solid solution region, therefore, can be obtained by shifting the $P(\text{Mg})$ calculated from Eq. 26 in the direction of the "pressure-axis" of the diagram for $\log P$ -vs.- n and joining it to the $P(\text{Mg})$ in the two-phase region. The results are shown in Fig. 9, along with the experimental values. The calculated values agreed with those obtained by

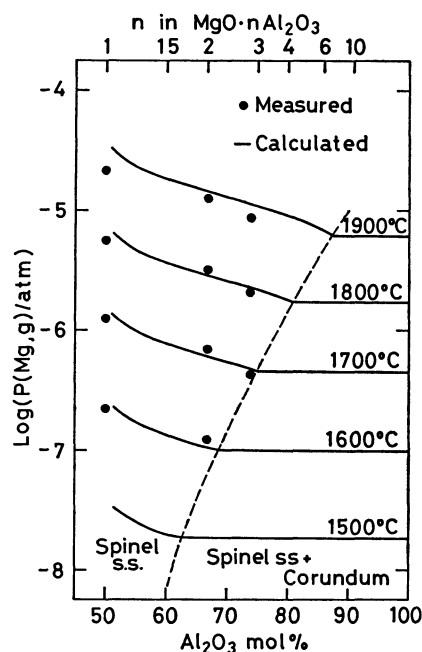


Fig. 9. Calculated and measured vapor pressures of $\text{Mg}(\text{g})$ over the system MgAl_2O_4 - Al_2O_3 .

mass spectrometry.

We would like to thank Mr. Ryoichi Kondoh of the Tokyo Denki Kagaku Co., Ltd., for his assistance in obtaining the mass-spectrometric data.

References

- 1) T. Sata and T. Yokoyama, *Yogyo Kyokai Shi*, **81**, 501 (1973).
- 2) E. Watanabe and M. Naito, "Recent Developments in Mass Spectrometry," ed by K. Ogawa and T. Hayakawa, University of Tokyo Press (1970), p. 249.
- 3) E. Watanabe, M. Naitoh, and T. Aoyama, *Kogyo Kagaku Zasshi*, **67**, 1778 (1964).
- 4) R. T. Grimley, "The Characterization of High-Temperature Vapors," ed by J. L. Margrave, John Wiley & Sons (1967), p. 222.
- 5) J. B. Mann, *J. Chem. Phys.*, **46**, 1646 (1967).
- 6) K. Shirasuka and G. Yamaguchi, *Yogyo Kyokai Shi*, **81**, 97 (1973); **82**, 650 (1974).
- 7) J. B. Berdowitz-Mattuck, A. Büchler, J. L. Engelke, and S. N. Goldstein, *J. Chem. Phys.*, **39**, 2722 (1963).
- 8) P. O. Scissel and O. C. Trulson, *J. Chem. Phys.*, **43**,

737 (1965).

9) J. Drowart, G. De Maria, R. P. Burns, and M. G. Inghram, *J. Chem. Phys.*, **32**, 1366 (1960).

10) J. Drowart, G. Exsten, and G. Verhaegen, *Trans. Faraday Soc.*, **60**, 1920 (1964).

11) T. Sasamoto, H.-L. Lee, and T. Sata, *Yogyo Kyokai Shi*, **82**, 603 (1974).

12) T. Sata and H.-L. Lee, *J. Am. Ceram. Soc.*, **61**, 326 (1978).

13) A. M. Alper, R. N. McNally, P. H. Ribble, and R. C. Doman, *J. Am. Ceram. Soc.*, **45**, 263 (1962).

14) D. M. Roy and E. F. Osborn, *J. Am. Ceram. Soc.*, **36**,

149 (1953).

15) JANAF Thermochemical Tables, 2nd ed.

16) R. L. Altman, *J. Chem. Phys.*, **67**, 366 (1963).

17) D. S. Rutman, I. L. Shchetnikova, E. I. Kelareva, and G. A. semenov, *Ogneupory*, No. 10, 40 (1968).

18) M. Nakano, *Yogyo Kyokai Shi*, **81**, 491 (1973).

19) K. Koumoto, S. Mizuta, and H. Yanagida, *Yogyo Kyokai Shi*, **83**, 217 (1980).

20) K. Shirasuka and G. Yamaguchi, *Yogyo Kyokai Shi*, **83**, 603 (1975).

21) K. Shirasuka, G. Yamaguchi, and M. Momoda, *Yogyo Kyokai Shi*, **84**, 523 (1976).
